



Original Article

Transplantation of human umbilical cord blood mononuclear cells promotes functional endometrium reconstruction via downregulating EMT in damaged endometrium

Ruomeng Hu ^{a, b, c, 1}, Ying Wang ^{a, b, c, 1}, Wenwen Li ^{a, b, c, 1}, Hongjiang Liu ^{a, b, c, 1},
Rong Wu ^{a, b, c}, Xuan Xu ^{a, b, c}, Xiaohua Jiang ^{a, b, c}, Qiong Xing ^{a, b, c}, Jianye Wang ^{a, b, c, *},
Zhaolian Wei ^{a, b, c, **}

^a Reproductive Medicine Center, Department of Obstetrics and Gynecology, The First Affiliated Hospital of Anhui Medical University, No 218 Jixi Road, Hefei 230022, Anhui, China

^b Anhui Province Key Laboratory of Reproductive Health and Genetics, Anhui Medical University, No 81 Meishan Road, Hefei 230032, Anhui, China

^c NHC Key Laboratory of Study on Abnormal Gametes and Reproductive Tract (Anhui Medical University), No 81 Meishan Road, Hefei 230032, Anhui, China

ARTICLE INFO

Article history:

Received 27 November 2023

Received in revised form

6 March 2024

Accepted 28 March 2024

Keywords:

Umbilical cord blood mononuclear cell
Endometrial injury
Epithelial-mesenchymal transition (EMT)
PTEN-AKT signaling pathway
Intrauterine adhesion

ABSTRACT

Introduction: Cell transplantation is an emerging and effective therapeutic approach for enhancing uterine adhesions caused by endometrial damage. Currently, human umbilical cord blood mononuclear cells (HUCBMCs) have been extensively used for tissue and organ regeneration. However, their application in endometrial repair remains unexplored. Our investigation focuses on the utilization of HUCBMCs for treating endometrial injury.

Methods: The HUCBMCs were isolated from healthy umbilical cord blood, and co-cultured with the injured endometrial stromal cells and injured endometrial organoids. The cell proliferation and apoptosis were measured by cck8 assays and flow cytometry. Western blotting was used to detect the expression of PTEN, AKT and p-AKT. Immunofluorescence assay revealed expression levels of epithelial-mesenchymal transition (EMT)-related markers such as E-cadherin, N-cadherin, and TGF- β 1. The endometrial thickness, fibrosis level, and glandular number were examined after the intravenous injection of HUCBMCs in mouse endometrial models. Immunohistochemistry was employed to assess changes in growth factors vascular endothelial growth factor (VEGF) and insulin-like growth factor 1 (IGF-1) as well as fibrosis markers α -SMA and COL1A1. Additionally, expressions of EMT-related proteins E-cadherin and N-cadherin were evaluated.

Results: HUCBMCs significantly improved the proliferation and reduced the apoptosis of damaged endometrial stromal cells (ESCs), accompanied by up-regulation of phospho-AKT expression. HUCBMCs increased endometrial thickness and glandular count while decreasing fibrosis and EMT-related markers in mouse endometrial models. Furthermore, EMT-related markers of ESCs and endometrial organoids were significantly decreased.

Conclusions: Our findings suggest that HUCBMCs plays a pivotal role in mitigating endometrial injury through the attenuation of fibrosis. HUCBMCs may exert a reverse effect on the EMT process during the endometrium reconstruction.

© 2024, The Japanese Society for Regenerative Medicine. Production and hosting by Elsevier B.V. This is an open access article under the CC BY-NC-ND license (<http://creativecommons.org/licenses/by-nc-nd/4.0/>).

* Corresponding author. Reproductive Medicine Center, Department of Obstetrics and Gynecology, The First Affiliated Hospital of Anhui Medical University, No 218 Jixi Road, Hefei 230022, Anhui, China.

** Corresponding author. Reproductive Medicine Center, Department of Obstetrics and Gynecology, The First Affiliated Hospital of Anhui Medical University, No 218 Jixi Road, Hefei 230022, Anhui, China.

E-mail addresses: Wangjianye9@126.com (J. Wang), weizhaolian_1@126.com (Z. Wei).

Peer review under responsibility of the Japanese Society for Regenerative Medicine.

¹ Ruomeng Hu, Ying Wang, Wenwen Li and Hongjiang Liu contributed equally to this work.

1. Introduction

Endometrial repair disorder following endometrial injury refers to the damage of the basal layer, resulting in fibrosis and intrauterine adhesions (IUA). Clinically, it is characterized by a thin endometrium, amenorrhea, and secondary infertility [1]. These conditions are associated with reduced endometrial receptivity, leading to decreased implantation rates and increased miscarriage risk. Despite various treatment approaches for thin endometrium such as medication and hysteroscopic surgery, hyperfibrotic or unresponsive cases often experience recurrent postoperative adhesions that do not respond adequately to estrogen therapy [2–4]. Therefore, there is a need for more effective strategies in managing endometrial repair disorders.

Cell transplantation is a new treatment to repair effect injured tissue such as heart, kidney, hepar and endometrium. Increasing number of scholars pay attention to the regeneration of damaged endometrium by cell transplantation. Mononuclear cells (MNCs) are used as a source of stem cell reservoir, which containing a high level of primitive multipotent stem cells, progenitor cells, monocytes and regulatory T cells. Three main types of single cells that have been studied and applied, namely, peripheral blood mononuclear cells (PBMNCs), bone marrow-derived mononuclear cells (BMMNCs), and umbilical cord blood mononuclear cells (UCBMCs) [5]. In previous clinical studies reported that human PB-MNCs transplantation could increase the thickness of the damaged endometrium, and exerted a positive influence on endometrial receptivity and embryonic implantation in mice [6,7]. Experts found umbilical cord blood could provide a sufficient number of stem cells with low tissue rejection, thus, human umbilical cord blood mononuclear cells (HUCBMCs) transplantation for tissue repairing became a promising effective treatment. Pre-clinical studies have demonstrated that transplantation of HUCBMCs could enhance functional recovery by promoting local angiogenesis and improving blood perfusion to the damaged areas in brain ischemia models [8,9].

The aim of this study was to assess the efficacy of HUCBMCs in restoring endometrial injury. Our results demonstrate that HUCBMCs effectively reverse endometrial damage and reverse EMT progression. These findings have significant implications for the clinical development of HUCBMC-based products for treating endometrial injuries.

2. Materials and methods

2.1. Isolation of human umbilical cord blood mononuclear cells

The human umbilical cords were obtained from healthy puerperas, while cord blood was collected from the punctured umbilical vein postpartum. All human-derived samples were collected with approval from the ethics review board of the First Affiliated Hospital of Anhui Medical University.

The cord blood was collected into a 50 ml centrifuge tube containing twice the volume of phosphate buffered saline (PBS) within 5 min. The mixed cord blood was then added to an equal volume of Ficoll-Hypaque Solution (Tianjinhaoyang, LTS1077, China). Mononuclear cells were isolated by centrifugation over a Ficoll-Hypaque density gradient at 600 rpm for 25 min at 4 °C. The cells at the interface were collected and centrifuged at 500 rpm for 5 min at 4 °C, followed by three washes with PBS and resuspension in Gibco Dulbecco's Modified Eagle Medium: F-12 (DMEM/F-12). The morphology of the resulting mononuclear cells was determined using Wright Giemsa staining.

2.2. Establishment of the damaged endometrial stromal cell model

Endometrial tissues were obtained from patients with histologically confirmed normal endometrium in the proliferative phase. The study protocol was approved by the Ethical Committee of Anhui Medical University (PJ2020-12-48), and written informed consent was obtained from all participants. A gentle endometrial scratching procedure was performed to enhance the success rate of embryo transfer. All enrolled individuals were healthy fertile women with regular menstrual cycles lasting 25–30 days, who had not used hormonal contraception, intrauterine devices, or undergone hormone therapy for at least 3 months prior to surgery. Endometrial cycle assessment, including evaluation of endometrial thickness (i.e., measurement of endometrial stripe) and pathological examination, was conducted based on comprehensive analysis of patient's menstrual history, B-sonography findings, and histological examination.

The fresh endometrial specimens in the proliferative phase were rinsed, minced into small pieces (1–2 mm³), and subsequently incubated with 0.1% type I collagenase (Sigma, C0130, USA). The dispersed endometrial cells were then separated by filtration through successive nylon sieves (180 μm and 40 μm nylon sieve). The small cells represent ESCs, while the large cells correspond to endometrial glandular epithelium cells. ESCs were cultured in DMEM/F-12 supplemented with 10% FBS (Gibco, USA) and 1% penicillin/streptomycin (Hyclone, USA).

The ESCs at passage 3–5 were harvested and plated at a density of 3×10^5 cells/ml in a 6-well plate, followed by a resting period of 48 h before stimulation. Following the 48-h resting period, the medium was replaced with serum-free medium to remove FBS. To induce injury in ESCs, the cells were treated with mifepristone (Sigma, USA) at a concentration of 60 μmol/L for 48 h. After treatment, fresh serum-free medium was used for further culturing. An in vitro model of ESCs injury was successfully established [10]. In the following experiments, untreated ESCs were categorized into the Fresh group, while mifepristone-induced injury model ESCs were classified as the Model group. Additionally, ESCs collected after co-culturing with HUCBMCs following mifepristone-induced injury model establishment were assigned to the HUCBMCs group.

2.3. Establishment of damaged endometrial organoid model

The endometrial glandular epithelium cells were derived from freshly collected endometrial tissue as previously described [11–13]. Subsequently, the cells were mixed with a uniform combination of 70% Matrigel in DMEM/F12 medium. A 30 μl volume of this mixture was then placed onto pre-warmed 48-well plates and allowed to solidify. After solidification, the human organoid culture medium was supplemented with N-acetyl-L-cysteine (1.25 mM; Sigma-Aldrich), the p38 inhibitor SB202190 (10 μM; Sigma-Aldrich), and 17β-estradiol (E2, 2 nM; Sigma-Aldrich). Additional components were incorporated into the EMO medium, which consisted of DMEM/F12 supplemented with 1% penicillin/streptomycin (Life Technologies), 2 mM Glutamax (Life Technologies), 2% B27 (Life Technologies), 1% N₂ (Life Technologies), 1% insulin-transferrin-selenium (ITS, Life Technologies), 1 mM nicotinamide (Sigma Aldrich), and growth factors including EGF at a concentration of 50 ng/ml (R&D Systems), FGF10 at a concentration of 50 ng/ml (Peprotech), Noggin at a concentration of 100 ng/ml (R&D Systems), TGFβ/Alk inhibitor A83-01 at a concentration of 0.5 μM (Tocris), and WNT activators WNT3A and RSPO1 added as conditioned medium (CM) in specified proportions. Cultures were

maintained under conditions of temperature at 37 °C in an incubator containing 5% CO₂, and the culture medium was refreshed every two days.

Once a stable culture for endometrial organoids is established, this model can be utilized to conduct investigations on endometrial glands. For establishing a human uterine organoid injury model, matured organoids were treated with mifepristone at a concentration of 60 μmol/L for 48 h and then cleared from the culture after an additional 48 h. This resulted in the successful establishment of a human uterine organoid injury model. In the following experiments, untreated uterine organoids were categorized into the Fresh group, while mifepristone-induced injury model uterine organoids were classified as the Model group. Additionally, uterine organoids collected after co-culturing with HUCBMCs following mifepristone-induced injury model establishment were assigned to the HUCBMCs group.

2.4. Co-culture experiment

To establish co-culture models of HUCBMCs with ESCs as well as HUCBMCs with endometrial organoids, we conducted experiments using transwell chambers (Corning Transwell; 3413; USA). The cell model to be treated was placed in a six-well culture dish. Once the damaged model was stabilized, 3 ml of serum-free DMEM-F12 was added to the culture dish, and the transwell chamber was inserted into the six-well dish. HUCBMCs were suspended in serum-free DMEM-F12 at a concentration of 5×10^5 cells/ml. Then, 2 ml of the HUCBMCs cell suspension was seeded in the upper chamber. Due to the permeability of the polycarbonate membrane at the bottom of the transwell chamber, HUCBMCs in the upper chamber could influence ESC or endometrial organoid models in the lower chamber.

2.5. Proliferation assay by cell counting kit 8 assay (CCK8)

The CCK-8 kit (Dojindo, Japan) was used to assess cell proliferation according to the manufacturer's instructions. Briefly, ESCs were seeded in 24-well plates with medium supplemented with 10% FBS and incubated at 37 °C for 24 h to allow adhesion. Subsequently, the serum-free medium containing 60 μmol/L mifepristone was replaced and cultured for an additional 48 h. DMEM/F-12 was then substituted as a control while co-culturing with HUCBMCs. Finally, the absorbance at 450 nm was measured using a microplate reader.

2.6. Flow cytometric analysis of cell apoptosis

The ESCs were harvested from 6-well culture plates, and the cultivation supernatant was aspirated to terminate cell growth. Subsequently, the cells were washed twice with PBS before being incubated in binding buffer containing FITC-conjugated Annexin V and propidium iodide (Vazyme Biotech Co., Ltd., China) for 15 min at room temperature under light-free conditions. Flow cytometry analysis (BD FACSCalibur, USA) was performed on the cells.

This assay enables discrimination of four distinct cell populations: intact cells (Annexin V-/PI-), early apoptotic cells (Annexin V+/PI-), necrotic cells (Annexin V-/PI+), and late-apoptotic/necrotic cells (Annexin V+/PI+). A total of ten thousand cells were routinely acquired, and the results were expressed as a percentage of Annexin V+ apoptotic and PI+ necrotic cells out of the total number of counted cells. Data analysis was conducted using Flowjo software.

2.7. Establishment of the mouse model

All experiments were conducted in accordance with the policies of the Animal Care and Use Committee at Anhui Medical University

(No. PJ2020-12-48), following approved protocols. C57BL/6 mice (The Anhui Medical University Laboratory) were housed in facilities provided by Anhui Medical University under direct veterinary supervision. The animals had unrestricted access to food and water in a temperature-controlled room, maintained on a 12-h light: 12-h dark illumination cycle.

The mice were randomly divided into three groups: the Sham operation group, IUA model group, and HUCBMCs treatment group. The mouse endometrial injury model was established using 95% alcohol by first opening the mouse abdomen under anesthesia to expose the uteri, followed by gentle injection of 95% ethanol into the uterine horn for a duration of 20 s to induce severe intrauterine adhesions [14]. Following the completion of ethanol treatment, the uterine horn was gently irrigated with a moderate volume of saline solution to remove any remaining ethanol. The mouse model of endometrial injury was established. In contrast, only normal saline solution was injected into the sham operation group. One week after modeling, the HUCBMCs treatment group received an intravenous injection of 5×10^5 HUCBMCs suspension via the tail vein. After one week, mice were euthanized and uterine tissues were collected.

2.8. Intracellular signaling evaluation by western blot analysis

Following appropriate periods of cultivation, ESCs were washed twice with PBS and then scraped into a lysate buffer containing 1 mM dithiothreitol (DTT), 1 mM phenylmethylsulfonyl fluoride (PMSF), 1 mg/ml leupeptin, 2 mg/ml aprotinin, and 5 mM EGTA in PBS. The cells were sonicated using a sonifier cell disrupter and the resulting sonicates were centrifuged at $10,000 \times g$ for 10 min. The supernatants were denatured in sample buffer and heated by boiling water for 5 min. The protein quantity was determined using a BCA protein assay kit (BioTeke Corporation, PP1001, China). Subsequently, the proteins were separated via 10% SDS-PAGE and electrophoretically transferred from the gels onto polyvinylidene difluoride (PVDF) transfer membranes. The membranes were blocked with 5% nonfat milk for 2 h, washed briefly in PBS-Tween, and then incubated overnight at 4 °C with primary antibodies against PTEN (1:1000, Cell Signaling, mAb #9559, USA), AKT (1:1000, Cell Signaling, mAb #4691, USA) and p-AKT (1:1000, Cell Signaling, mAb #4060, USA). An appropriate secondary antibody was applied for an additional 2-h incubation period, followed by protein expression evaluation using the Bio-Rad Imaging System (Bio-Rad Biosciences, USA), with GAPDH (1:1000, Cell Signaling, mAb #5174, USA) serving as an internal control for protein loading.

2.9. Immunofluorescence

After culturing the samples for an appropriate duration. Cells or organoids were fixed in 4% PFA for 30 min at room temperature and washed twice in PBS. Primary antibodies were incubated in blocking buffer with 0.05% Triton at 4 °C overnight. The details of the primary antibodies utilized in immunofluorescence studies are as follows: N-cadherin (1:200, Cell Signaling, mAb# 13,116, USA), E-cadherin (1:200, Cell Signaling, mAb# 24E10, USA), TGF-β(1:200, Cell Signaling, mAb# #3711, USA). Negative controls were prepared by omitting primary antibody. Cells or organoids were washed 3 times for 15 min in PBS. Cells or organoids were incubated for 3 h at room temperature in PBS with secondary antibodies: Alexa Fluor 488 goat anti-mouse IgG (1:1000, Abcam, ab150077, USA) and DAPI (Sigma, D9542, USA). Cells or organoids were washed in PBS for 30 min 3 times, mounted in confocal dish (Biosharp, BS-15-GJM, China) and imaged using the ZEISS 700 Confocal microscope and ZEN Microscope Software.

2.10. Hematoxylin-eosin (HE) staining

The uteri were fixed in a 4% paraformaldehyde solution for 24 h and subsequently embedded in paraffin using conventional methods. Serial sections (4 μm thick) were obtained from the paraffin-embedded samples. These sections were then sequentially dewaxed in xylene I and xylene II for 20 min each, followed by rehydration using a series of ethanol solutions with decreasing concentrations (100% for 10 min, 95% for 5 min, 90% for 5 min, 80% for another 5 min, and finally, 70% for an additional 5 min). Next, the sections underwent three rinses in distilled water lasting 5 min each before being stained with an H&E solution according to the manufacturer's instructions provided by Servicebio (China). The inverted microscope was utilized to observe any morphological changes in the endometrium. A transverse section of the uterus was taken to clearly display the widest part of the uterine cavity line and measure the thickness of double-layered endometrium on opposite sides. Additionally, gland numbers per unit area of endometrium were calculated based on observations made within five randomly selected high-power fields on each slide.

2.11. Masson staining

The uteri paraffin sections, measuring 4 μm in thickness, were subjected to dewaxing and rehydration procedures as previously described. Subsequently, a Masson staining kit from Servicebio (China) was used for staining according to the manufacturer's instructions. Briefly, the sections were immersed in Masson A solution overnight and then rinsed briefly under running water. Following this, a mixture of Masson A and Masson B solutions (1:1) was applied for 1 min before another rinse under running water. To enhance signal differentiation, the sections were briefly treated with 1% hydrochloric acid alcohol for 10 s prior to further washing. Next, immersion in Masson D solution occurred for 6 min followed by staining with Masson E solution for 1 min. The excess solution was gently drained off before placing the sections directly into Masson F solution for a period ranging from 2 to 30 s; subsequently, they were rinsed using a 1% glacial acetic acid solution. Dehydration was achieved through treatment with absolute ethyl alcohol while clarification involved exposure to xylene lasting approximately 5 min. Finally, the slides were sealed using Permount mounting medium. Evaluation of endometrial fibrosis levels involved randomly selecting five fields on each slide and calculating fibrotic percentages using Image-pro plus software (Media Cybernetics, USA).

2.12. Immunohistochemistry

The endometrial mouse tissues were fixed in 4% paraformaldehyde (Biosharp, BL539A, China) and subsequently embedded in paraffin. Following the kit instructions, tissue sections were cut into 5- μm thickness and stained with hematoxylin and eosin or Masson's Trichrome (Solarbio, G1340, China). The sections were then dewaxed by three immersions in histoclear for 10 min each before rehydration with 100%, 70%, and 50% IMS as well as dH_2O for 5 min each. Finally, the sections were incubated overnight at 4 °C with primary antibodies (diluted in antibody diluent reagent solution) The sections were subsequently incubated with HRP-conjugated secondary antibodies (1:1000, Abcam, ab150077, UK) at room temperature for 8 min. Afterward, DAB substrate (Solarbio, DA1010, China) was utilized to visualize the antigen signals and hematoxylin was used as a counterstain. The sections were then examined under a microscope (DMI8, Leica, Germany), and optical densities were quantified using Image-pro plus software (Media Cybernetics, USA). The list of antibodies employed in IHC is

provided below: CDH2/N-cadherin (1:200, Abcam, ab18203, UK), CDH1/E-cadherin (1:400, Abcam, ab76055, UK), α -SMA (1:200, Abcam, ab7817, UK), Smad2/3 (1:200, ABclonal, A11498, China), VEGF (1:200, Abcam, ab52917, UK), IGF-1 (1:200, Abcam, ab9572, UK).

2.13. Statistical analysis

The mean values with standard deviation were analyzed using GraphPad Prism6.02 (GraphPad Software Inc., San Diego, USA). The data obtained in this study were derived from a minimum of three independent experiments. The data are presented as the mean \pm standard deviation from at least three independent runs, and statistical analyses were performed using Student's two-tailed paired *t*-test. A *p*-value of less than 0.05 was considered statistically significant, indicated by an asterisk (*) for *p* < 0.05, two asterisks (**) for *p* < 0.01, three asterisks (***) for *p* < 0.005 and four asterisks (****) for *p* < 0.001.

3. Results

3.1. HUCBMCs protect ESCs from mifepristone-induced apoptosis by activating AKT pathways in vitro

To assess the impact of HUCBMCs on damaged ESCs, we evaluated the proliferation of ESCs using the CCK-8 assay. The confluent population of damaged cells reduced to approximately 30% in the Model group (Fig. 1A). A confluent population reaching around 50% in the HUCBMCs group. The density of ESCs was significantly higher in the HUCBMCs group compared to the Model group. The proliferation rates for two groups, with significantly higher rates observed in the HUCBMCs group compared to those in the Model group (Fig. 1B). Statistical analysis revealed a significant difference between these two groups. These findings suggest that HUCBMCs could enhance cell proliferation in damaged ESCs.

To further investigate the impact of HUCBMCs on damaged ESCs, we evaluated cell apoptosis and wound closure kinetics. Based on Annexin-V-FITC/PI staining and FACS analysis, the percentages of viable cells and apoptotic cells in the Fresh group were 96.5% and 2.1%, respectively. The percentage of living cells in the Model group was 70.5%, with an apoptotic cell rate of 22.4%. In contrast, the HUCBMCs group had corresponding rates of 86.6% and 9.13%, respectively. Additionally, there was a significant difference in the percentage of apoptotic cells between the HUCBMCs and Model groups (*p* < 0.01) (Fig. 1D). These results demonstrated a significant decrease in the apoptosis rate of ESCs with HUCBMCs treatment. Subsequently, an analysis was conducted on the migratory potential of ESCs in response to the influence exerted by HUCBMCs. In the presence of HUCBMCs, ESCs exhibited enhanced wound closure kinetics. At 24-h, co-cultured ESCs achieved a significantly higher extent of wound closure ($66.60\% \pm 2.441\%$) compared to the control group scratch assays ($27.20\% \pm 1.685\%$). Moreover, the scratches had healed in the HUCBMCs group by 48 h (Fig. 2A and B). Consequently, HUCBMCs facilitated the migration of ESCs.

The PTEN/AKT signaling pathways play a crucial role in regulating cell apoptosis and angiogenesis. The expression of phospho-AKT was significantly decrease in the Model group compared to the Fresh group (*p* < 0.01). Furthermore, HUCBMCs treatment led to a significant up-regulation of phospho-AKT expression when compared to the Model group (*p* < 0.01). However, no alteration was observed in AKT expression levels during our experiments (*p* > 0.05). Notably, we found a strong inverse correlation between PTEN and phospho-AKT expression (Fig. 2C and D). These findings suggest that HUCBMCs induce overexpression of phospho-AKT. Furthermore, it is likely to impact the associated pathways of

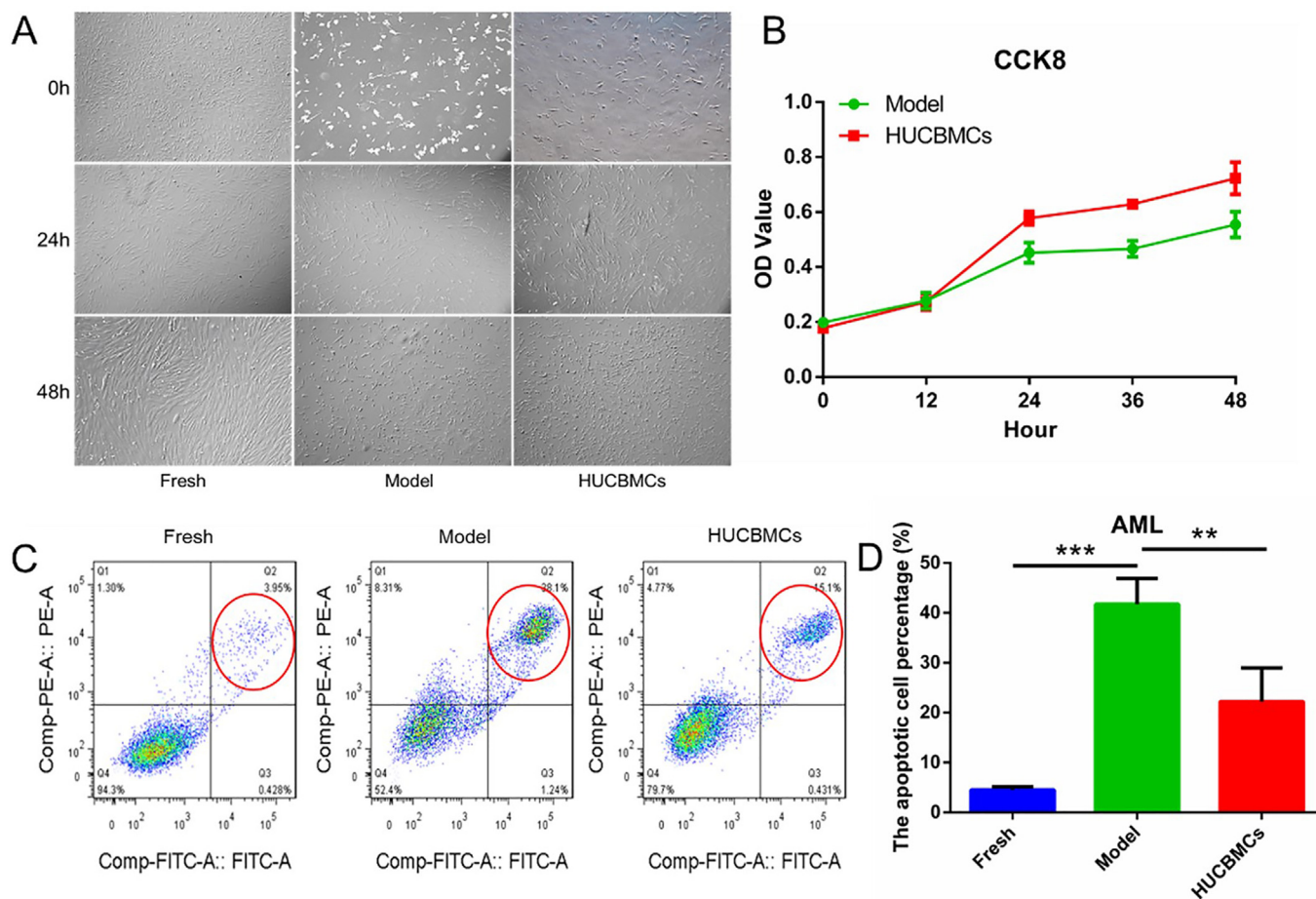


Fig. 1. HUCBMCs protect ESCs from mifepristone-induced apoptosis. **A** The morphology of ESCs in the Fresh group, Model group, and HUCBMCs group was examined using a light microscope at 0 h, 24 h, and 48 h, respectively (Original magnification $\times 100$). **B** The CCK8 assay demonstrates significantly higher proliferation rates in the HUCBMCs group compared to those in the Model group. **C, D** The Fresh group exhibited a viability rate of 96.5% and an apoptotic cell percentage of 2.1%, as determined by Annexin-V-FITC/PI staining and FACS analysis. In the model group, the proportion of viable cells was 70.5%, accompanied by an apoptotic cell rate of 22.4%. Conversely, the HUCBMCs group demonstrated corresponding rates of 86.6% and 9.13%. Statistical significance: $***p < 0.01$; $****p < 0.005$.

phosphorylated AKT and potentially influence the expression of certain growth factors, as evidenced by subsequent experiments and in line with our previous findings.

3.2. HUCBMCs promote the endometrial recovery and suppress fibrosis in mouse endometrial injury model

Histological examination of HE-stained tissues in the mouse model group revealed a significant reduction in endometrial thickness, accompanied by a shortened cuboidal epithelium and a loosely arranged matrix (Fig. 3A). Additionally, the glandular epithelium and endometrial epithelial cells exhibited shortened and flattened shapes. Mild edema was observed in certain regions of the matrix, with most areas displaying sparse blood vessels while others exhibited limited cellular structural outlines. The HUCBMCs group demonstrated an increase in endometrial thickness (Fig. 3B), glandular density (Fig. 3C), and a morphology more closely resembling that of the Sham operation group, suggesting that HUCBMCs could enhance the recovery of endometrium.

Immunohistochemical analysis of VEGF and IGF-1 demonstrated the presence of brown-yellow granules in the cytoplasm of glandular epithelial cells and stromal cells in mice from the Sham operation group. In the IUA model group, a significant decrease in

IGF-1 levels was observed ($p < 0.01$), while VEGF levels remained unchanged in endometrial tissue ($p > 0.05$) (Fig. 4A). Conversely, treatment with HUCBMCs resulted in an increased abundance of brown-yellow granules observed both in the endometrial glandular epithelium and stroma. A significant up-regulation in the expression of VEGF ($p < 0.001$) and IGF-1 ($p < 0.01$) within the injured endometrium after treatment with HUCBMCs (Fig. 4B and C). These suggest that HUCBMCs significantly up-regulated the expression of growth factors following endometrial damage.

Masson staining revealed that in the Sham operation group, the endometrial collagen fibers exhibited a blue hue and were arranged in an orderly fashion, while the mucosa, submucosa, muscles, and blood vessels displayed a red coloration. In the HUCBMCs treatment groups, there was a decrease in both the area ratio of blue-stained collagen fibers in endometrial mesenchymal and fibrosis area, with only a small amount of blue collagen fibers present in the interstitial region that were evenly arranged (Fig. 5A). Meanwhile, immunohistochemistry analysis revealed that the expression levels of fibrosis markers α -SMA and COL1A1 were significantly elevated in the model group compared to those in the sham operation group. However, following HUCBMCs treatment, a significant reduction was observed in both α -SMA ($p < 0.001$) and COL1A1 ($p < 0.05$) expression levels (Fig. 5B–D). These results suggest that HUCBMCs could reverse endometrial fibrosis.

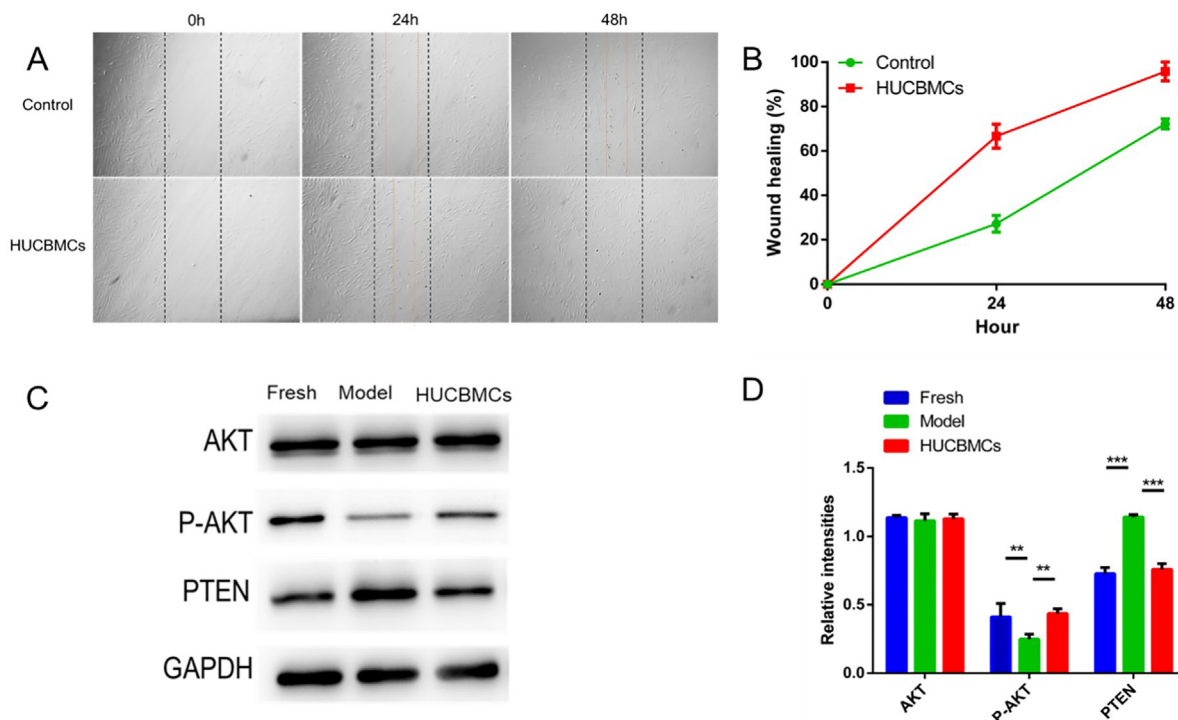


Fig. 2. HUCBMCs promote wound healing in ESCs and increase the expression of phospho-AKT, while decreasing PTEN expression. A Wound healing assays were conducted on ESCs co-cultured with HUCBMCs, as well as on control cells cultured without HUCBMCs. Phase-contrast images were captured at 0 h, 24 h, and 48 h post-scratching to obtain representative images (Original magnification $\times 100$). B The wound healing areas quantitatively analyzed using ImageJ software, and the corresponding data relative to the initial time point (0 h) were presented in the graph. Statistical significance was determined by *t*-test analyses with a threshold of $p < 0.001$. C, D Western blot was used to identify the expression of AKT, P-AKT, PTEN and GAPDH. Lanes 1, 2, and 3 represent the Fresh group, Model group, and HUCBMCs group. Statistical significance: ** $p < 0.01$; *** $p < 0.005$.

3.3. HUCBMCs reverse EMT of endometrial injury model

The visualization of target factors on endometrial organoids and ESCs was achieved through immunofluorescence analysis. Confocal

laser scanning microscopy revealed a distinct emission of bright fluorescence from the proteins E-cadherin, N-cadherin, and TGF β 1. ESCs exhibited an upregulation of N-cadherin ($p < 0.005$) accompanied by elevated TGF β 1 expression ($p < 0.001$) after mifepristone

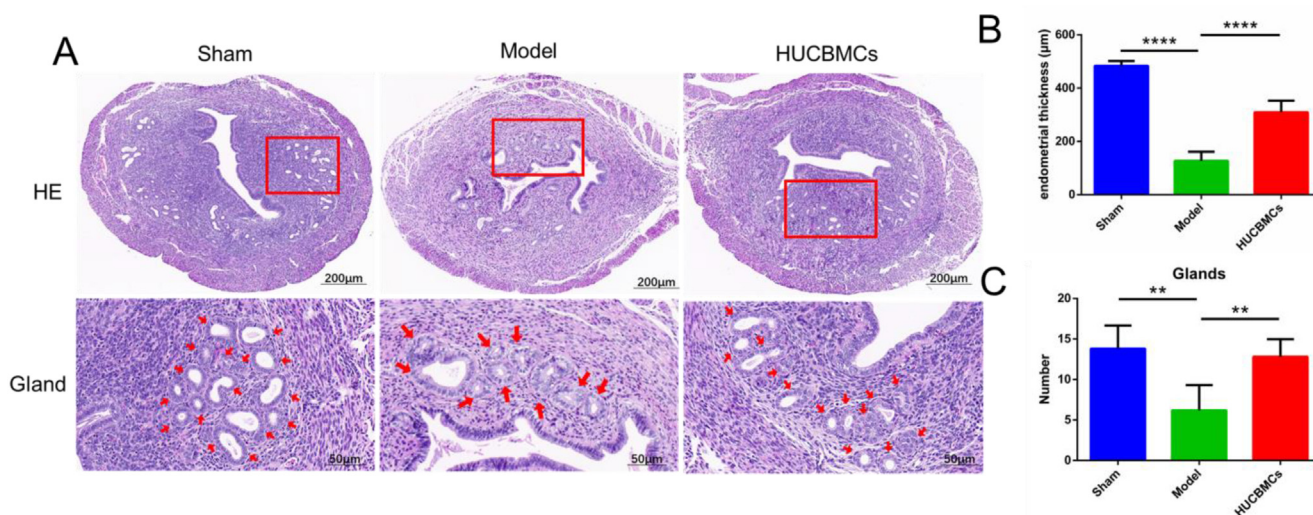


Fig. 3. HUCBMCs treatment significantly increased endometrial thickness and gland count, indicating its potential therapeutic effect on endometrial damage. A HE staining was performed to detect endometrial gland changes in the sham operation group, model group, and HUCBMCs group. B Statistical analysis revealed a significant reduction in endometrial thickness in the IUA model group compared to the sham operation group ($p < 0.001$), while the HUCBMCs group exhibited a significantly higher endometrial thickness than the IUA model group ($p < 0.001$). C Statistical results demonstrate a significant difference in gland number following endometrial damage and treatment ($p < 0.01$). The observed differences were compared with both the Sham operation group and IUA model group, as well as the IUA model group and HUCBMCs group ($p < 0.01$). Original magnification $\times 10$; Scale bar = 200 μ m; Statistical significance: ** $p < 0.01$; **** $p < 0.001$.

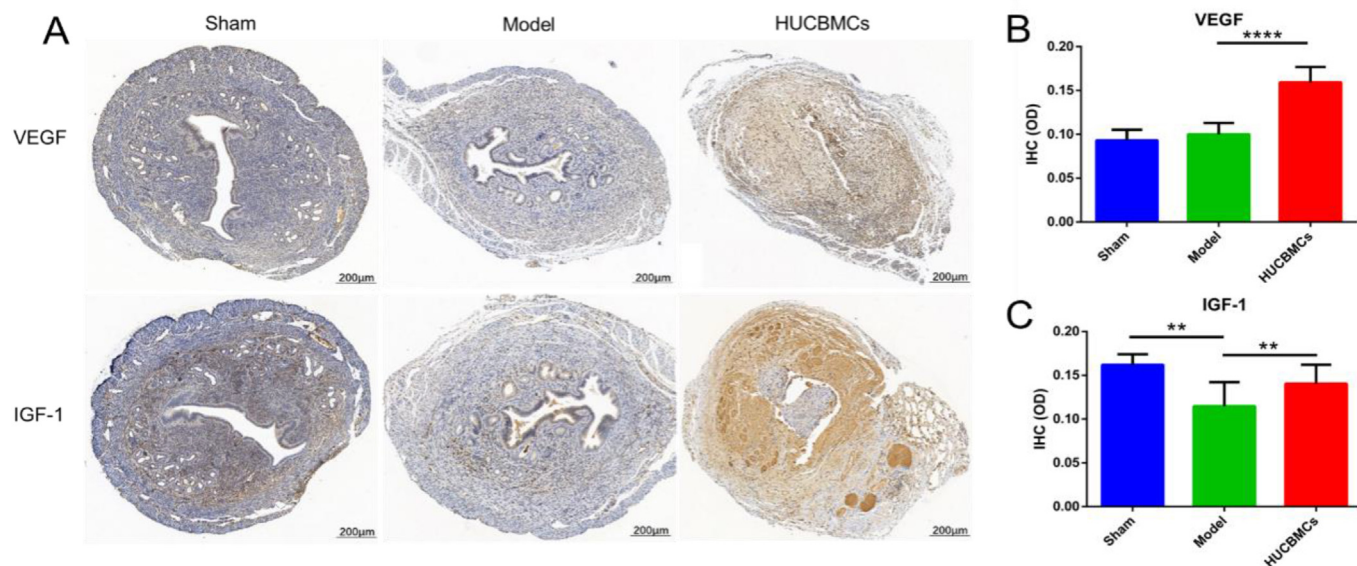


Fig. 4. HUCBMCs significantly up-regulated the expression of VEGF and IGF-1 in endometrium. A The expression of VEGF and IGF-1 were measured by immunohistochemical staining in the sham operation group, model group, and HUCBMCs group. B, C IUA model group exhibited a significant decrease in IGF-1 levels compared to the sham operation group ($p < 0.01$), while VEGF levels remained unchanged in endometrial tissue ($p > 0.05$). Conversely, treatment with HUCBMCs resulted in an upregulation of both VEGF ($p < 0.001$) and IGF-1 ($p < 0.01$) expression within the endometrium following treatment with HUCBMCs. Original magnification $\times 10$; Scale bar = 200 μm ; Statistical significance: ** $p < 0.01$; *** $p < 0.001$.

treatment. However, treatment with mifepristone only resulted in a slight increase in E-cadherin expression for ESCs, as untreated ESCs showed minimal or no expression of E-cadherin (Fig. 6A–D). Endometrial organoids were self-organized from endometrial glandular epithelium cells. Endometrial organoids were established and identified (Fig. S1A–C). There was a significant decrease in the expression of E-cadherin ($p < 0.001$) and a slight increase in N-cadherin ($p < 0.01$) observed in endometrial organoids after mifepristone treatment (Fig. 6E–G). These findings suggest that mifepristone can induce EMT in both ESCs and endometrial organoids, but the two models emphasize different aspects of EMT-related factors.

Immunofluorescence results of the HUCBMCs group showed that in the ESCs model, compared to the Model group, the HUCBMCs group exhibited a significant increase in E-cadherin expression ($p < 0.001$) and a significant decrease in N-cadherin expression ($p < 0.001$). Moreover, there was a decreased expression of TGF β 1 ($P < 0.005$) (Fig. 6A–D). In the endometrial organoids model, under the treatment of HUCBMCs, there was also a significant increase in E-cadherin expression ($p < 0.005$), while only a slight decrease in N-cadherin expression ($p < 0.05$) was observed (Fig. 6E–G).

Immunohistochemical staining was performed on uterine tissue sections following induced damage to the uterus. E-cadherin, N-cadherin, and Smad2/3 proteins exhibited a brown color on the cell membrane in the endometrium. The results demonstrated a significant decrease in E-cadherin expression ($p < 0.01$) and a notable increase in N-cadherin expression ($p < 0.01$) in the model group compared to the Sham group (Fig. 7B and C). Additionally, there was a substantial increase in Smad2/3 expression within the endometrium ($p < 0.05$) (Fig. 7D). Treatment with HUCBMCs resulted in an increase in E-cadherin expression ($p < 0.05$) and a decrease in N-cadherin expression ($P < 0.01$). Furthermore, there was a significant reduction observed in Smad2/3 expression ($p < 0.01$) within the endometrium (Fig. 7B and C). This finding is consistent with previous immunofluorescence analysis, which demonstrated concordant TGF- β expression.

4. Discussion

Currently, the treatment for endometrial injury involves hysteroscopic surgery combined with estrogen therapy; however, this approach has a high recurrence rate and diminishes endometrial receptivity [15]. Therefore, it is important to explore a safe and efficacious treatment for patients with intrauterine adhesions.

The endometrium affected by uterine adhesion presents two primary issues: tissue fibrosis and impaired endometrial cellular proliferation. Uterine infusion with bone marrow mesenchymal stem cells enhances endometrium thickness and up-regulates the expression of cytokeratin, vimentin, integrin $\alpha\beta\gamma$ 3, and LIF in the endometrium. This suggests that stem cell therapy not only facilitates endometrial regeneration but also improves endometrial receptivity [16,17]. However, traditional stem cell therapy relies on laboratory-cultured stem cells and their derived products. This will result in an inadequate supply of cells, thereby posing challenges to the stability and continuity of long-term treatment with stem cells. HUCBMCs are more readily accessible and easier to prepare compared to processed and ex vivo expanded MSCs [18]. Mesenchymal stromal cells resulted in a higher incidence of severe complications (mortality, ocular inflammation) compared to HUCBMCs in stroke treatment, suggesting that the latter may be a safer option [19].

In our study, we have confirmed that HUCBMCs significantly enhance the growth of ESCs and glandular cells, and HUCBMCs have the potential to enhance endometrial healing and improve endometrial thickness, possibly mediated through the PTEN/AKT signaling pathway. The findings were further validated through animal experimentation, where in mice treated with HUCBMCs exhibited a significant increase in endometrial thickness and gland, inhibited endometrial fibrosis. Our data demonstrate higher expression of VEGF and IGF-1, along with lower expression of α -SMA and COL1A1 in the HUCBMCs transplanted rats, suggesting that HUCBMCs therapy not only facilitates endometrial regeneration but also mitigates endometrial fibrosis.

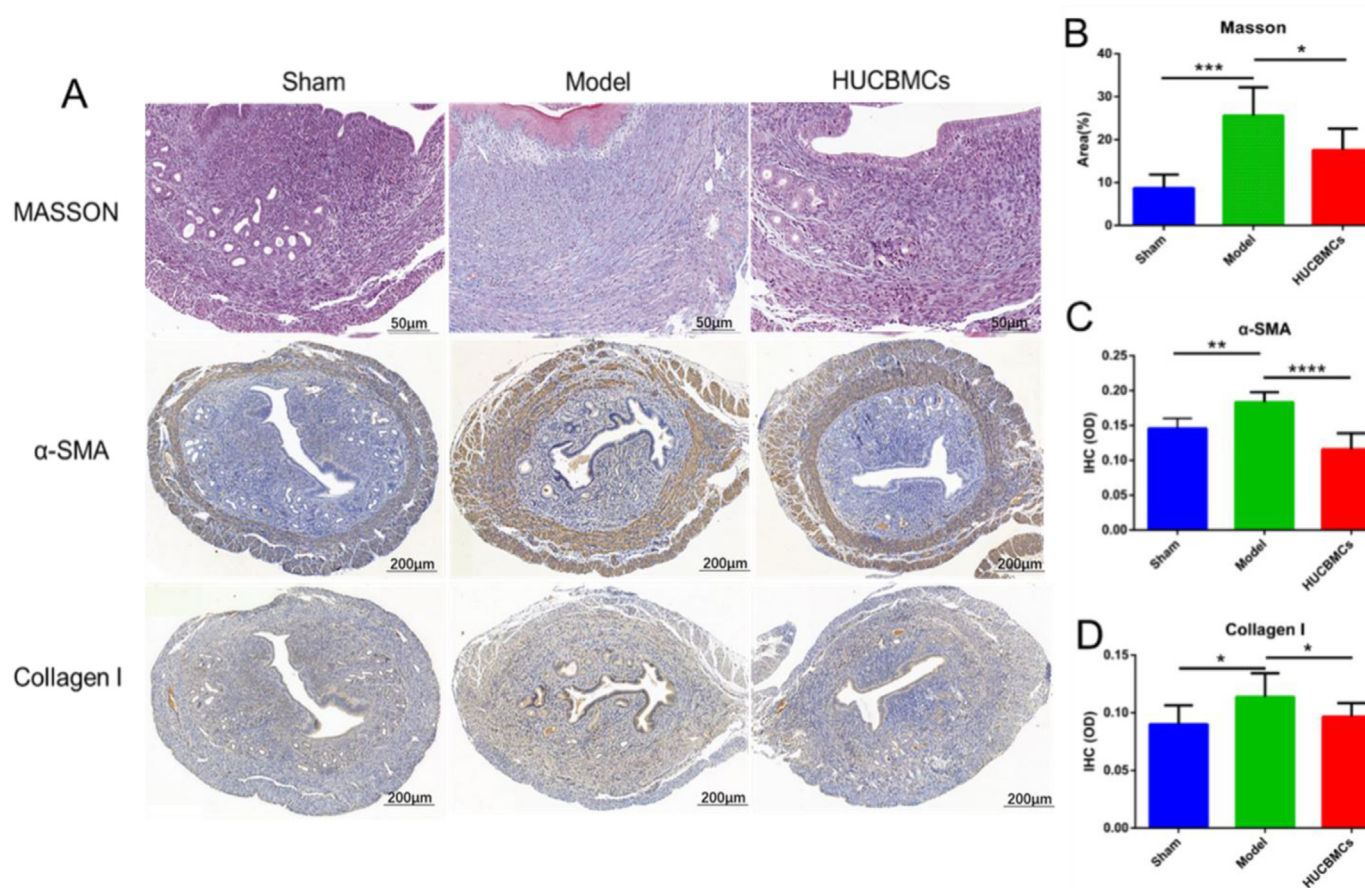


Fig. 5. HUCBMCs effectively mitigate intrauterine fibrosis in endometrial damage. A Masson staining, α -SMA, Collagen I was performed to detect intrauterine fibrosis changes in each group. Original magnification $\times 40$; Scale bar = 50 μ m. B, C, D Statistical results of intrauterine fibrosis changes after endometrial damage and treatment. The observed differences were compared with the IUA model group and HUCBMCs group ($p < 0.05$). Expression levels of fibrosis markers α -SMA and COL1A1 were significantly higher in the model group compared to those in the sham operation group. However, following treatment with HUCBMCs, a significant decrease was observed in both α -SMA ($p < 0.001$) and COL1A1 ($p < 0.05$). Original magnification $\times 10$; Scale bar = 200 μ m; Statistical significance: * $p < 0.05$; ** $p < 0.01$; *** $p < 0.005$; **** $p < 0.001$.

Previous studies have demonstrated that the CD34⁺ cell population, enriched in HUCBMCs [20], comprises endothelial progenitor cells capable of inducing angiogenesis in ischemic tissues. We propose that CD34⁺ progenitors with endothelial from HUCBMCs developmental potential are recruited to injury sites and undergo differentiation into new endometrial cells, thereby facilitating tissue repair or sprouting novel vascular structures. Additionally, CD34⁺ cells and hematopoietic precursors secrete various angiogenic factors including VEGF, hepatocyte growth factor (HGF), and IGF-1 [21]. The exosomes secreted by CD34⁺ cells carry a plethora of proteins, micro-RNAs, which can attenuate apoptosis and promote cellular proliferation.

EMT is known to play a major role in most fibrotic diseases [22], and it is believed to be a fundamental mechanism underlying IUA. Exosomes derived from MSCs enhanced endometrial receptivity through the reversal of EMT [23]. Exploring strategies to impede EMT in endometrium may present a novel approach towards addressing and managing IUA. Our results suggest that HUCBMCs effectively reverse the EMT process in damaged endometrium.

TGF- β 1 plays a distinct role in the development and progression of IUAs, as it is one of the key factors involved in inducing EMT. Additionally, it facilitates fibroblast and inflammatory cell aggregation, promotes collagen and fibrin synthesis, leading to extracellular matrix deposition and degradation. The severity of IUAs positively correlates with the expression levels of TGF- β 1 and

Smad3 [24,25]. Research findings suggest that miRNA-29b and miRNA-326 have the potential to alleviate endometrial fibrosis in primary human endometrial stromal cells by significantly reducing COL1A1 and α -SMA expression through inhibition of the TGF- β 1/Smad signaling pathway [26].

In this study, mifepristone was employed to establish in vitro cell models, including an ESCs injury model and endometrial organoid injury model. Following the establishment of these models, the expression intensity of E-cadherin and N-cadherin was assessed using immunofluorescence analysis. E-cadherin, a transmembrane protein, is ubiquitously expressed in epithelial cells and mediates homotypic cell-cell adhesion, playing a pivotal role in maintaining the structural integrity of epithelial tissues. The initiation and key event during EMT involve the down-regulation of E-cadherin. In contrast, N-cadherin is predominantly expressed in mesenchymal cells, indicating an up-regulation of EMT [23]. Alterations in N-cadherin were observed in the ESC model, while changes in E-cadherin were more pronounced in the endometrial organoid model. These findings suggest that mifepristone can effectively induce an in vitro endometrial EMT model. Comparative analysis with the sham operation group revealed a significant decrease in E-cadherin expression and a significant increase in N-cadherin expression in mice models, indicating a substantial enhancement of ethanol-induced endometrial EMT in mice.

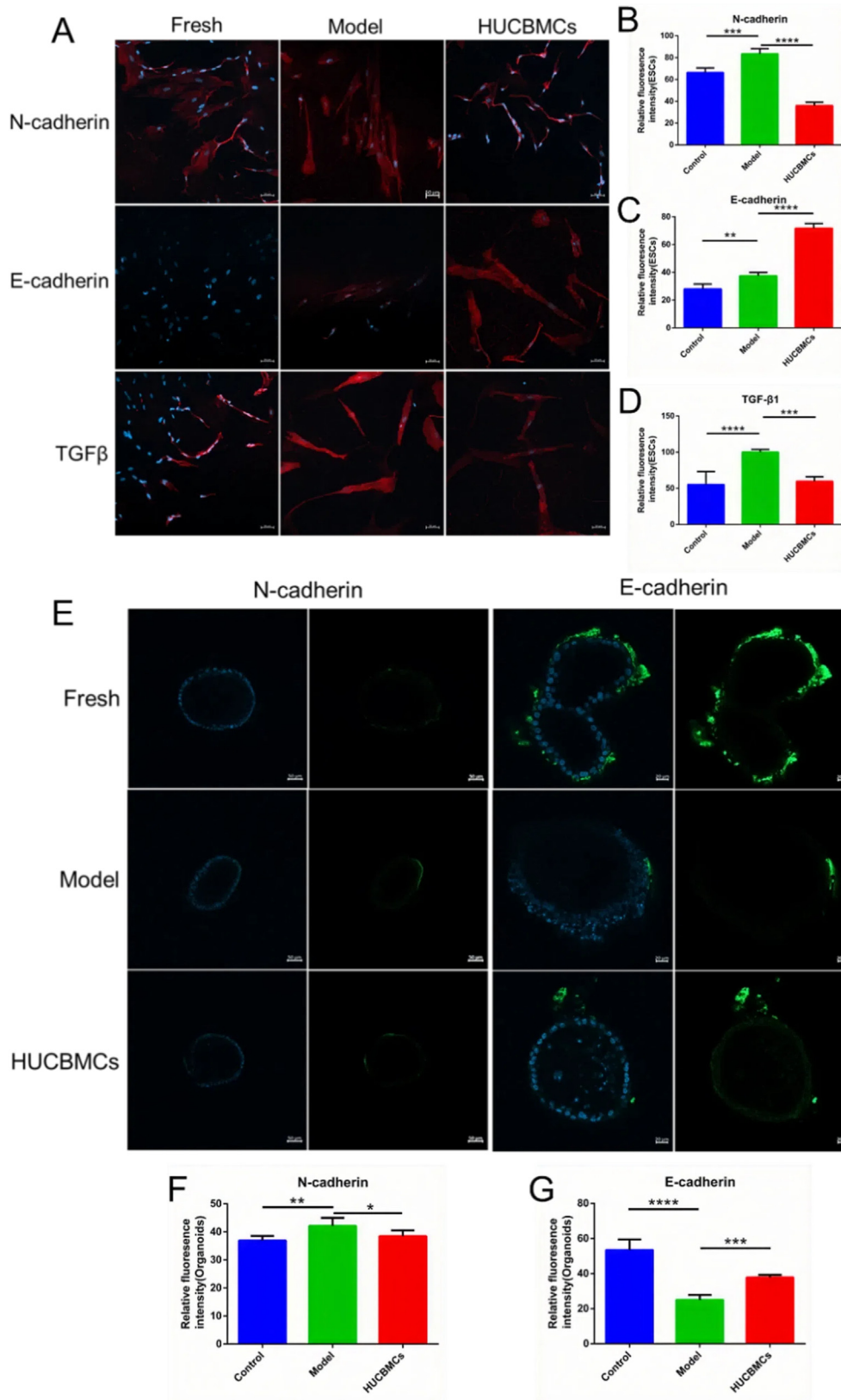


Fig. 6. HUCBMCs reverse EMT of endometrial injury model in vitro. A-D Immunofluorescence analysis revealed a significant upregulation of E-cadherin expression ($p < 0.001$) and a significant downregulation of N-cadherin ($p < 0.001$) expression in the HUCBMCs group compared to the Model group in ESCs model. Furthermore, there was a notable decrease observed in TGFβ1 expression ($p < 0.005$). E-G In the model of endometrial organoids, treatment with HUCBMCs resulted in a significant upregulation of E-cadherin expression ($p < 0.005$) and only a slight downregulation of N-cadherin expression ($p < 0.05$). Original magnification $\times 100$; Scale bar = 50 μm ; Statistical significance: * $p < 0.05$; ** $p < 0.01$; *** $p < 0.005$; **** $p < 0.001$.

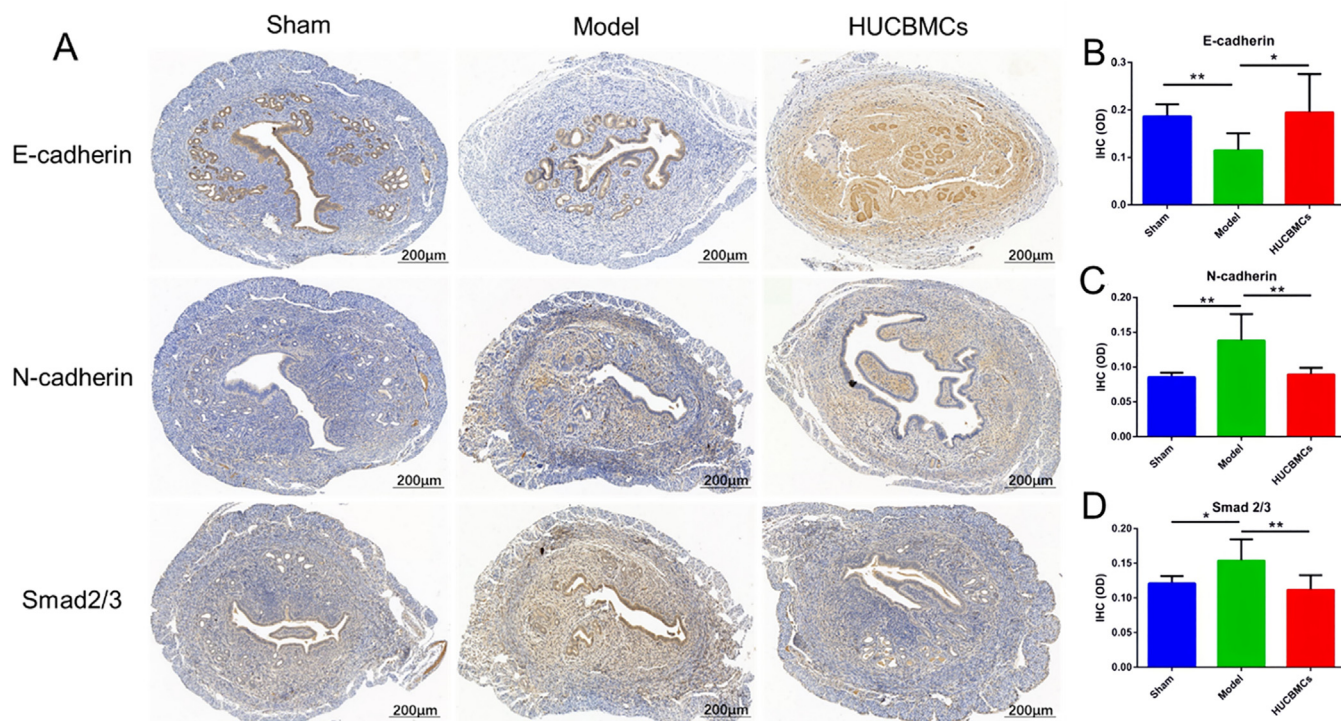


Fig. 7. HUCBMCs reverse EMT of IUA endometrium in vivo. **A** The expression of E-cadherin, N-cadherin and Smad2/3 were measured by immunohistochemical staining in the sham operation group, model group, and HUCBMCs group. **B, C, D** A significant downregulation of E-cadherin expression ($p < 0.01$) and a notable upregulation of N-cadherin expression ($p < 0.01$) in the model group compared to the Sham group. Moreover, there was a substantial increase in Smad2/3 expression within the endometrium ($p < 0.05$). Treatment with HUCBMCs led to an upregulation of E-cadherin expression ($p < 0.05$) and a decrease in N-cadherin expression ($p < 0.01$). Furthermore, there was a significant reduction observed in Smad2/3 expression within the endometrium ($p < 0.01$). Original magnification $\times 10$; Scale bar = 200 μm ; Statistical significance: * $p < 0.05$; ** $p < 0.01$.

After treatment with HUCBMCs in both in vitro and animal models, we observed an up-regulation of E-cadherin expression and a down-regulation of N-cadherin expression compared to the injury model. These results demonstrated that HUCBMCs effectively reversed the EMT process in damaged endometrium, as evidenced by in vitro experiments using both ESCs and endometrial organoids, as well as animal experiments conducted on mouse endometrium. Thus, HUCBMCs effectively reversed the EMT process in damaged endometrium.

The process of EMT is a complex biological phenomenon that may involve the activation of multiple signaling pathways. The activation and expression of transcription factors that induce EMT are observed in response to various signaling pathways, including those mediated by transforming growth factor β (TGF- β), bone morphogenetic protein (BMP), epidermal growth factor (EGF), fibroblast growth factor (FGF), platelet-derived growth factor (PDGF), Wnt, Sonic Hedgehog (Shh), Notch, and integrin signaling [15,22,27,28]. There is a strong correlation between the TGF- β /Smad signaling pathway and the development of endometrial fibrosis. In this study, it was observed that the expression of Smad2/3 in the endometrium of mice significantly increased following exposure to alcohol compared to the Sham operation group. Conversely, treatment with HUCBMCs resulted in a significant downregulation of protein expressions of Smad2/3 when compared to the injured endometrium group. This suggests that the repair of endometrial fibrosis may be associated with the TGF- β 1/Smad signaling pathway, and that HUCBMCs may regulate the fibrosis repair of injured endometrium by downregulating the TGF- β 1/Smad signaling pathway. The precise mechanism remains unclear and further investigation is warranted.

This study represented the potential therapeutic effects of HUCBMCs to damaged endometrium through reversing EMT in endometrial cells. We employed not only the conventional in vitro culture of ESCs and animal experimentation but also utilized a novel cell experimental platform comprising endometrial organoids. However, further investigation is warranted to elucidate the specific active substance within HUCBMCs or adhesion molecule on its surface that plays a pivotal role in this process.

5. Conclusion

This study demonstrates the effective promotion of endometrial repair by HUCBMCs through enhanced cell regeneration and reduced apoptosis. Furthermore, it has been confirmed that HUCBMCs significantly mitigate fibrosis in damaged endometrium both in vitro and in vivo. Additionally, our findings elucidate the role of HUCBMCs-mediated reversal of impaired endometrial EMT, thereby highlighting its potential application in the prevention and treatment of intrauterine adhesions.

Data availability statement

The unique findings generated in this research are incorporated within the article material, for additional queries please contact the corresponding author.

Ethics statement

All animal experiments and procedures were approved by Anhui medical University Ethics Committee.

Author contributions

Ruomeng Hu, Ying Wang and Wenwen Li conducted the experiments, analyzed the data, prepared figures, and contributed to drafting or reviewing the paper. Other authors were responsible for material preparation and experimental work. Zhaolian Wei and Jianye Wang conceived and designed the experiments. All authors critically reviewed the manuscript and agreed to take responsibility for its content.

Funding

This work was supported by grants from National Natural Science Foundation of China (No. 82171619), Anhui Provincial Health Research Project (No. AHWJ2023A20010) and Anhui Provincial Natural Science Foundation for Universities (No. 2022AH051193).

Declaration of competing interest

All authors declare no conflicts of interest.

Appendix A. Supplementary data

Supplementary data to this article can be found online at <https://doi.org/10.1016/j.reth.2024.03.030>.

References

- Metello JL, Jimenez JF. Intrauterine adhesions: etiopathogenesis. In: Tinelli A, Alonso Pacheco L, Haimovich S, editors. *Hysteroscopy*. Cham: Springer International Publishing; 2018. p. 691–6.
- Li XC, Liang CX, Li J, Li PF, Zhao Y. Effect of hysteroscopic adhesiolysis combined with growth hormone on endometrial blood flow and volume as well as Smad2/3 expression. *J Hainan Med Univ* 2016;22:98–101.
- Salma U, Xu D, Sheikh SA. Observational study of new treatment proposal for severe intrauterine adhesion. *Int J Biosci* 2011;1:43–56.
- Zhou X. Application of estradiol valerate in severe intrauterine adhesions after hysteroscopic adhesiolysis. *Sichuan J Physiol Sci* 2014;2:64–6.
- Xi Y, Yue G, Gao S, Ju R, Wang Y. Human umbilical cord blood mononuclear cells transplantation for perinatal brain injury. *Stem Cell Res Ther Sep* 5;2022;13:458.
- Ahn JY, Hong YH, Kim KC, Kim JH, Lee SY, Lee JR, et al. Effect of human peripheral blood mononuclear cells on mouse endometrial cell proliferation: a potential therapeutics for endometrial regeneration. *Gynecol Obstet Invest* 2022;87:105–15.
- Yu N, Yang J, Guo Y, Fang J, Yin T, Luo J, et al. Intrauterine administration of peripheral blood mononuclear cells (PBMCs) improves endometrial receptivity in mice with embryonic implantation dysfunction. *Am J Reprod Immunol Jan*;2014;71:24–33.
- Peterson DA. Umbilical cord blood cells and brain stroke injury: bringing in fresh blood to address an old problem. *J Clin Invest Aug*;2004;114:312–4.
- Park DH, Borlongan CV, Willing AE, Eve DJ, Cruz LE, Sanberg CD, et al. Human umbilical cord blood cell grafts for brain ischemia. *Cell Transplant* 2009;18:985–98.
- Wang J, Hu R, Xing Q, Feng X, Wei Z. Exosomes derived from umbilical cord mesenchymal stem cells alleviate mifepristone-induced human endometrial stromal cell injury. *Stem Cells International Jan*;2020;1–9. 6091269.
- Boretto M, Cox B, Noben M, Hendriks N, Fassbender A, Roose H, et al. Development of organoids from mouse and human endometrium showing endometrial epithelium physiology and long-term expandability. *Development May* 15;2017;144:1775–86.
- Turco MY, Gardner L, Hughes J, Cindrova-Davies T, Gomez MJ, Farrell L, et al. Long-term, hormone-responsive organoid cultures of human endometrium in a chemically defined medium. *Nat Cell Biol May*;2017;19:568–77.
- Jiang X, Li X, Fei X, Shen J, Chen J, Guo M, et al. Endometrial membrane organoids from human embryonic stem cell combined with the 3D Matrigel for endometrium regeneration in asherman syndrome. *Bioact Mater Nov*;2021;6:3935–46.
- Zhang S, Sun Y, Jiang D, Chen T, Liu R, Li X, et al. Construction and optimization of an endometrial injury model in mice by transcervical ethanol perfusion. *Reprod Sci Mar*;2021;28:693–702.
- Yang JH, Chen CD, Chen SU, Yang YS, Chen MJ. The influence of the location and extent of intrauterine adhesions on recurrence after hysteroscopic adhesiolysis. *Bjog Mar*;2016;123:618–23.
- Wu M, Li Y, Yang W, Ma B, Sun L, Xie J. Progress on the clinical applications of stem cells for thin endometrium. *Nano LIFE* 2020;10:2040001. 2020/03/01.
- Zhao J, Zhang Q, Wang Y, Li Y. Uterine infusion with bone marrow mesenchymal stem cells improves endometrium thickness in a rat model of thin endometrium. *Reprod Sci Feb*;2015;22:181–8.
- Rodrigues LP, Iglesias D, Nicola FC, Steffens D, Valentim L, Witczak A, et al. Transplantation of mononuclear cells from human umbilical cord blood promotes functional recovery after traumatic spinal cord injury in Wistar rats. *Braz J Med Biol Res Jan*;2012;45:49–57.
- Karlupia N, Manley NC, Prasad K, Schäfer R, Steinberg GK. Intraarterial transplantation of human umbilical cord blood mononuclear cells is more efficacious and safer compared with umbilical cord mesenchymal stromal cells in a rodent stroke model. *Stem Cell Res Ther Apr* 1;2014; (5):45.
- Hildbrand P, Cirulli V, Prinsen RC, Smith KA, Torbett BE, Salomon DR, et al. The role of angiopoietins in the development of endothelial cells from cord blood CD34+ progenitors. *Blood Oct* 1;2004;104:2010–9.
- Majka M, Janowska-Wieczorek A, Ratajczak J, Ehrenman K, Pietrzakowski Z, Kowalska MA, et al. Numerous growth factors, cytokines, and chemokines are secreted by human CD34(+) cells, myeloblasts, erythroblasts, and megakaryoblasts and regulate normal hematopoiesis in an autocrine/paracrine manner. *Blood May* 15;2001;97:3075–85.
- Caja L, Dituri F, Mancarella S, Caballero-Diaz D, Moustakas A, Giannelli G, et al. TGF- β and the tissue microenvironment: relevance in fibrosis and cancer. *Int J Mol Sci Apr* 26;2018;19:1294.
- Yao Y, Chen R, Wang G, Zhang Y, Liu F. Exosomes derived from mesenchymal stem cells reverse EMT via TGF- β /Smad pathway and promote repair of damaged endometrium. *Stem Cell Res Ther Jul* 29;2019;10:225.
- Li J, Du S, Sheng X, Liu J, Cen B, Huang F, et al. MicroRNA-29b inhibits endometrial fibrosis by regulating the Sp1-TGF- β /Smad-CTGF axis in a rat model. *Reprod Sci Mar*;2016;23:386–94.
- Salma U, Xue M, Ali Sheikh MS, Guan X, Xu B, Zhang A, et al. Role of transforming growth factor- β 1 and smads signaling pathway in intrauterine adhesion. *Mediat Inflamm* 2016;2016:4158287.
- Ning J, Zhang H, Yang H. MicroRNA-326 inhibits endometrial fibrosis by regulating TGF- β 1/Smad3 pathway in intrauterine adhesions. *Mol Med Rep Aug*;2018;18:2286–92.
- McCormack N, O'Dea S. Regulation of epithelial to mesenchymal transition by bone morphogenetic proteins. *Cell Signal Dec*;2013;25:2856–62.
- Espinoza I, Miele L. Deadly crosstalk: Notch signaling at the intersection of EMT and cancer stem cells. *Cancer Lett Nov* 28;2013;341:41–5.